Crystal structure of calcium dodecin (Rv0379), from Mycobacterium tuberculosis with a unique calcium-binding site

ARTICLE *in* PROTEIN SCIENCE · MAY 2011

Impact Factor: 2.85 · DOI: 10.1002/pro.607 · Source: PubMed

5 AUTHORS, INCLUDING:

Arockiasamy Arulandu
International Centre for Genetic Engineering a…
18 PUBLICATIONS **362** CITATIONS
SEE PROFILE

Andreas Holzenburg
Texas A&M University
140 PUBLICATIONS **2,993** CITATIONS
SEE PROFILE

Crystal structure of calcium dodecin (Rv0379), from *Mycobacterium tuberculosis* with a unique calcium-binding site

Arulandu Arockiasamy,[1] Anup Aggarwal,[1] Christos G. Savva,[2] Andreas Holzenburg,[2] and James C. Sacchettini[1,3]*

[1]Department of Biochemistry and Biophysics, Texas A&M University, College Station, Texas 77843-2128
[2]Microscopy and Imaging Center and Department of Biology, Texas A&M University, Biological Sciences Building West, College Station, Texas 77843-2257
[3]Center for Structural Biology, Institute of Biosciences and Technology, Houston, Texas 77030

Received 10 November 2010; Accepted 1 February 2011
DOI: 10.1002/pro.607
Published online 2 March 2011 proteinscience.org

Abstract: In eukaryotes, calcium-binding proteins play a pivotal role in diverse cellular processes, and recent findings suggest similar roles for bacterial proteins at different stages in their life cycle. Here, we report the crystal structure of calcium dodecin, Rv0379, from *Mycobacterium tuberculosis* with a dodecameric oligomeric assembly and a unique calcium-binding motif. Structure and sequence analysis were used to identify orthologs of Rv0379 with different ligand-binding specificity.

Keywords: calcium-binding; dodecin; *Mycobacterium tuberculosis*; dodecamer; bidentate binding; distorted hexagonal bipyramid

Introduction

Calcium is a ubiquitous secondary messenger that controls a variety of cellular processes in eukaryotes[1,2] and therefore calcium-binding proteins (CaBPs) play a key role in signaling and regulating different stages of the eukaryotic cell cycle. During this process, CaBPs bind calcium with either an EF-hand[3] or a non-EF-hand motif.[4] Although eukaryotic equivalents of CaBPs in prokaryotes remain virtually unexplored, emerging evidence suggests the involvement of calcium in several diverse cellular processes in bacteria.[5–8] Furthermore, the presence of calmodulin-like protein sequences with an EF-hand motif suggests a possible role for calcium in signaling and regulation in bacteria.[9–12] A CaBP has not been identified or characterized in *Mycobacterium tuberculosis* (*Mtb*). The *Mtb* Rv0379, a 71 amino acid and 8 kDa protein, belongs to the family of conserved small molecular weight (~8 kDa) proteins containing about 70 amino acids (Pfam: DUF1458 and COG3360) and unknown *in vivo* function. The crystal structure identified *Mtb* Rv0379 as a calcium dodecin (Ca dodecin) and reveals a calcium-binding motif not observed in any other CaBP. Among Mycobacteria, the gene encoding Ca dodecin is present only in *Mtb* and its closest relative *Mycobacterium bovis*, suggesting a possible role in their intracelluar life cycles.

Results and Discussion

Ca dodecin was crystallized as an oligomer with 12 molecules in the asymmetric unit. The structure of

Additional Supporting Information may be found in the online version of this article.

Coordinates for Ca dodecin have been submitted to PDB with the ID: 3ONR.

Grant sponsor: National Institutes of Health; Grant number: P01AlO68135; Grant sponsor: Robert A. Welch Foundation; Grant number: A-0015.

Arulandu Arockiasamy's current address is International Centre for Genetic Engineering and Biotechnology (ICGEB), Aruna Asaf Ali Marg, New Delhi 110067, India.

*Correspondence to: James C. Sacchettini, Department of Biochemistry and Biophysics, Texas A&M University, 2128 TAMU, Room 218, College Station, TX 77843-2128, USA. E-mail: sacchett@tamu.edu

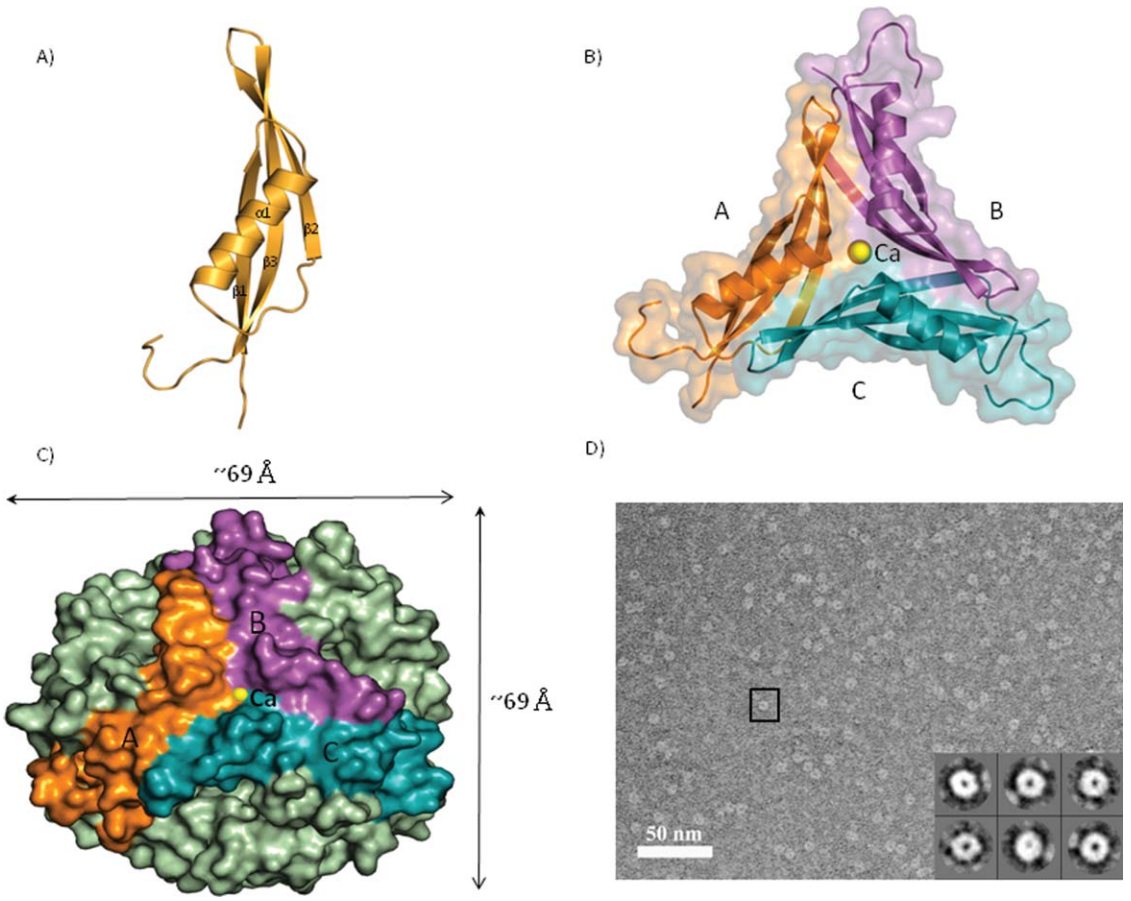

Figure 1. Structural organization of Ca dodecin. The crystal structure of Ca dodecin from monomeric and oligomeric forms are shown. (A) Ribbon representation of subunit A. (B) The trimer is shown in ribbon representation with the molecular surface in the background. The central calcium is in yellow. Subunits, A, B, and C are color coded orange, pink, and cyan, respectively. (C) Surface representation of the dodecameric oligomer in light green. One of the four trimers in the oligomer is colored as in Panel B. Water molecules, including the ones that were bound to calcium, have been removed to show the presence of calcium at the trimer interface. (D) Single-particle analysis of Ca dodecin. Electron micrograph of Ca dodecin single particles is shown. One of the Ca dodecin single particles in the micrograph is boxed. Scale bar corresponds to 50 nm. The inset in the micrograph depicts characteristic class averages after reference-free classification. The box size is 16.5 nm.

the monomeric Ca dodecin [Fig. 1(a)] follows a simple β1-α1-β2-β3 architecture, with the SHS2 configuration conserved in a variety of proteins with diverse functions such as protein-protein interactions, small molecule recognition, and catalysis.[13] All three strands form a twisted β-sheet with a groove with which the hydrophobic side of the amphipathic helix interacts. The overall three-dimensional architecture of the Ca dodecin oligomer is similar to the *Halobacterium salinarum* dodecin (hsDodecin), a riboflavin-binding protein involved in riboflavin homeostasis.[14–17] The three subunits bind one calcium ion at the interface [Fig. 1(b)], and the association of four equivalent sets of three subunits and a calcium leads to dodecameric oligomerization [Fig. 1(c)]. Subunit association is facilitated by an extensive backbone hydrogen bonding network, leading to the formation of an extended anti-parallel β-sheet at the subunit–subunit interface of the trimer. The residues Arg36-Val40 (head) of the β2 strand from one subunit associates with the Asn43-Val47 residues (tail) of the β2 strand of the neighboring subunit, resulting in a head-to-tail arrangement of the subunits. The majority of the interactions between the three subunits involve eighteen inter-subunit backbone hydrogen bonds (6/interface). The subunit–subunit interface is 27.1 Å long and 18.4 Å wide, and 42% of the residues in each subunit are involved in trimer formation. The 22–26 Å diameter cavity present inside the oligomeric assembly contains several ordered water molecules. In addition to the dodecameric crystal structure, data from single particle electron microscopy (EM) [Fig. 1(d)] and dynamic light scattering (DLS) further validate the oligomeric assembly in solution. The spherical particles observed in EM images are about 75 Å in diameter

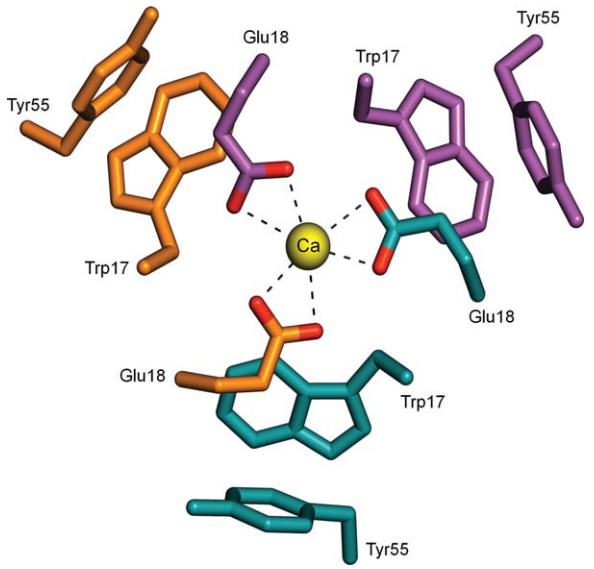

Figure 2. The unique calcium-binding site. The core residues Trp17, Glu18, and Tyr55 of the calcium-binding pocket at the Ca dodecin trimer interface are shown. The three bidentate forks of Glu18 clamp down one calcium ion (yellow) at the center. The residues are colored according to the subunit they belong to in the trimer, as shown in Figure 1. Only the backbone atoms are shown.

which agrees with the hydrodynamic radius (68–70 Å) obtained from DLS studies, as well as the crystal structure [Fig. 1(c)].

Glu18 from each Ca dodecin subunit provides the carboxylate group that binds calcium in a bidentate fashion. The bulky aromatic side chains of Trp17 and Tyr55 form a base for the calcium-binding pocket [Fig. 2(a)]. Three consecutive alanines (Ala20, 21, 22), along with Tyr55, complete the hydrophobic pocket around the three Glu18 residues that bind calcium at the center (Supporting Information Fig. S1). Overall, the core of the Ca-binding pocket is negatively charged with hydrophobic surroundings and extensive secondary and outer shell interactions stabilize the calcium-binding site (Supporting Information Fig. S2(a,b)). Additionally, the three bidentate carboxylates, along with two water molecules, form a distorted hexagonal bipyramid coordination geometry with all six carboxylate oxygens covering the base of the bipyramid and the water molecules occupying the two apical sites (Supporting Information Fig. S3(a,b)). Thus, the coordination number (CN) for the bound calcium in Ca dodecin is 8. The average bond length of 2.4–2.7 Å between the carboxylate oxygen atoms of Glu18 and the central calcium corroborates with the bidentate binding mode [Fig. 2(b)].[18–21] The angle (O–Ca–O) between two Ca–O bonds in Glu18 carboxylate, 49.6° to 52.2°, supports the reported value of ~50.0° for bidentate binding.[18,21] Also, the angles of Ca-$OE^{1,2}$-C^{γ}, 87–98°, in the Glu18 carboxylate are closer to the values known in other small molecule calcium chelating complexes (80°–100°), and are unlike the values for monodentate ligands which range between 110°–140°. The distance between the bidentate carboxylate oxygen atoms of two adjacent Glu18 residues is 2.9–3.0 Å in this "triple-fork" type ligand coordination. Therefore, as expected, the bidentate binding of Glu18 carboxylate oxygens distorts the geometry from the ideal hexagonal bipyramid.[21] The interplanar angle between two bidentate carboxylates and the central calcium is ~68°–75°, and as opposed to monodentate binding, this distorted geometry has been observed with bidentate chelating mode at a higher coordination number (CN) that accommodates more ligands.[21] While only a few proteins have calcium with CN-8, a majority of CaBPs show CN 6 to 7 with octahedral or pentagonal bipyramidal coordination geometry (http://tanna.bch.ed.ac.uk/). However, water molecules are often major coordinating ligands in CaBPs with CN-8.

The presence of calcium in native Ca dodecin purified from *E. coli* (125 mM of calcium/626 mM of protein) without any tag was confirmed by Inductively Coupled Plasma Optical Emission Spectroscopy (ICP-OES). For the His-tag removed Ca dodecin sample, an excess amount of calcium was added, passed through a gel-filtration column, and dialyzed against a buffer containing chelex-100 resin to remove all the unbound calcium before ICP-OES analysis. The molar ratio of calcium to protein in this sample is 0.39:1, which agrees with the amount of calcium observed in the high-resolution crystal structure (0.33:1). However, the calcium removed apo protein forms a dodecameric structure, but the oligomer dissociates into trimers upon crystallization at acidic pH 4.5 (data not shown), indicating that oligomerization does not require the presence of calcium.

Although Ca dodecin and hsDodecin share low sequence identity, their overall structure is very similar (Supporting Information Fig. S4) with RMSDs of 1.23 Å and 1.17 Å for the protomer and trimer, respectively. Essentially, these dodecins are the smallest dodecameric structures known to date. Two other small molecular weight (~100 a.a.) hypothetical proteins from the pathogenic bacteria *Bacillus cereus* and *Shigella flexneri* also share a very similar tertiary structure (PDB:1VR4 and 1Y2I) at the monomeric level (RMSD = 1.83, 1.73 Å over 51 and 40 C^{α} atoms, respectively). However, these proteins form a pentameric oligomer with a narrow channel at the center, and neither can form a Ca dodecin-like dodecameric assembly due to an extended N-terminus and a long insertion (~30 amino acids) between β1 and α1. A similar fold was detected in the N-terminal dimerization domain (RMSD = 1.9 Å over 36 residues) of lysine 5, 6-aminomutase (PDB:

1XRS, residues 33–84), a protein that is involved in lysine catabolism.[22] The fold of the dodecin subunit is also similar to the copper-binding domain (CuBD) of an Alzheimer's disease amyloid precursor protein (PDB: 1OWT), which is a neuronal regulator of copper homeostasis[23] with no apparent sequence identity (RMSD = 7.66 Å over 59 C^{α} atoms). Based on the hits from a similarity search, a structural motif containing a three-stranded twisted β-sheet and an amphipathic α-helix is present in several proteins with varying functions, and is not restricted to riboflavin-binding or calcium-binding dodecamers.[13] It is apparent that the functional annotation of Ca dodecin (Rv0379) as "SecE2" with possible involvement in protein secretion, based on 30% sequence identity with the γ-subunit of an archean translocase, does not seem to be correct from the structural viewpoint. Also, with an inner chamber diameter of 22–26 Å that has no noticeable features for a chaperone or translocase accessory molecule, the direct involvement of Ca dodecin in protein secretion seems far less feasible.

Detailed comparison of Ca dodecin and flavin binding dodecin structures suggests that many features of the calcium-binding pocket in Ca dodecin are, in part, preserved in hsDodecin, except for Trp17 and the bidentate ligand Glu18. However, among three residues that bind riboflavin in hsDodecin, Trp36 and Gln55 are conserved in several other putative dodecins, and the Glu45 is replaced by His/Gln/Thr amino acids, but are not conserved in Ca dodecin and its homologs, suggesting a specific requirement for riboflavin binding. Multiple sequence alignment (Supporting Information Fig. S5a, S5b) with nonredundant members of the family resulted in the observation of subclasses that are potentially dodecins with diverse ligand specific motifs: the first subgroup contains Ca dodecin-like proteins with a conserved calcium-binding sequence motif. The second subgroup has orthologs of hsDodecin with residues conserved consistent with the riboflavin-binding motif, and the third group, surprisingly, possesses calcium-binding ligand Glu in addition to riboflavin-binding residues. Regardless of sequence similarity (20%–59% identity), all the members of this family are expected to share an overall three-dimensional fold, like Ca dodecin and hsDodecin. Although the biological function of Ca dodecin is yet to be determined, identification of Ca dodecin as an immunodominant sero-antigen emphasizes a possible role in host response.[24,25] The antigenicity of Ca dodecin and its use in detecting *Mtb*-specific sera from TB patients[26] also suggests that Ca dodecin could be a secreted or shed antigen.[27,28] In addition, the characteristics of the calcium-binding pocket in Ca dodecin suggest that the dodecins could be used as a scaffold to create custom designed metal and flavin binding sites.

Materials and Methods

Cloning and purification of Ca dodecin

The gene for Ca dodecin (Rv0379) was PCR amplified using H37Rv genomic DNA as template (produced through funds from the National Institutes of Health, National Institute of Allergy and Infectious Diseases, contract N01-AI-75320) and cloned into the NcoI and HindIII sites of pET28b (Novagen) expression vector. The 3′ PCR primer included a stop codon at the end of the gene to avoid a C-terminal His-tag. This construct had no additional tags. To get a His-tagged version of Rv0379, the PCR fragment was cloned into the NdeI and HindIII sites of pET28b. The plasmid containing the Ca dodecin gene was used to transform the *E. coli* strain Rosetta (DE3) pLysS (Novagen) and grown in LB media supplemented with kanamycin (50 mg/L) and chloramphenicol (34 mg/L). The cells were grown at 37°C to an OD_{600} of ~1.0 and then induced with 0.5 mM of IPTG at 18°C for 12–14 hours. The bacterial culture was harvested by centrifugation at 4°C, 4000 rpm for 45 min and stored at −20°C. For protein purification, the cell pellet was resuspended in a buffer containing 25 m*M* Tris-HCl pH 8.0, 10 m*M* NaCl, 1 m*M* PMSF (phenylmethylsulphonyl fluoride), and 10 m*M* $MgCl_2$. DNase-I was added (20 μg/g of cell pellet) and lysed by passage through a French press cell (Thermo Scientific) at ~11,000 psi. The cell lysate was spun at 40,000 rpm for 1 hour (Beckman rotor Ti50.2), and the resulting supernatant was passed through a Q-sepharose column and eluted with a NaCl gradient of 10–500 m*M*. Ca dodecin eluted between 40 and 75 m*M* NaCl concentration and the fractions enriched in Ca dodecin were pooled, concentrated, and dialyzed against a buffer containing 25 m*M* Tris-HCl pH 8.0 and 10 m*M* NaCl. The His-tagged version of Ca dodecin was expressed and purified to homogeneity using Ni^{2+}-chelating sepharose and the tag was removed using thrombin before further characterization.

Crystallization, structure solution, and refinement

Native Ca dodecin was crystallized in several conditions of commercially available screens, like crystal screens I and II (Hampton Research). Crystals were obtained in the condition containing 1*M* sodium formate and 10 m*M* $CaCl_2$ (as additive). X-ray data sets were collected from the SBC-CAT 19ID and BioCARS-CAT 14BM-C, 14ID-B, and CAM-CAT 23-ID beam lines at the Advanced Photon Source of Argonne National Laboratory (Chicago). Crystals were mounted on a cryostream either straight from the drop or soaked in a reservoir containing a higher concentration of sodium formate for cryoprotection. Crystals of Ca dodecin diffracted beyond 1.8 Å and belonged to the $P2_12_12_1$ space group with cell

Table I. *Data Collection and Refinement Statistics of Ca Dodecin Rv0379 from Mtb*

Data collection	
Space group	$P2_12_12_1$
Unit-cell parameters (Å)	70.19, 78.45, 152.49
Resolution range (Å)	76.7–1.8
No. of reflections	147,741
Unique reflections	78,323
R_{sym} a (%)	2.7 (23.9)
I/σ (I)	20.8 (6.0)
Completeness (%)	99.1 (97.6)
Redundancy	1.9
Refinement	
Resolution (Å)	76.7–1.8
No. of reflections	74,344
R_{work}/R_{free} (%)	18.4/23.2
No. of atoms	
Overall	6863
Protein	6382
Ligand/ions	43
Waters	438
Average B factor (Å2)	
Overall	16.8
Protein	14.2
Waters	21.3
R.m.s. deviations	
Bonds (Å)	0.03
Angles (°)	2.02
Ramachandran	
Most favored (%)	90.9
Additionally allowed (%)	8.3
Generously allowed (%)	0.7

dimensions: $a = 70.19$ Å, $b = 78.45$ Å, $c = 52.49$ Å, and $\alpha = \beta = \gamma = 90°$. Data sets were indexed and scaled using HKL2000.[29] Multiwavelength anomalous dispersion (MAD)[30] phasing, from diffraction data collected (Table I) for a native crystal soaked with K_2-Pt$(CN)_4$ was used to obtain an initial electron density map. The following computational crystallographic programs were used to get the final refined model: (1) SHELXD,[31] to find initial heavy atom sites, (2) AutoSHARP,[32] for heavy atom refinement and to get initial phases and solvent flattened electron density map, (3) Xtalview,[33] for manual model building, (4) CNS,[34] for rigid body refinement and simulated annealing at the initial stage of model building, (5) Refmac5,[35] for restrained refinement (6) Shake&wARP,[36] for bias removed electron density map, and (7) CCP4 suite,[37] for refinement using Refmac5 with TLS parameters and for the use of other crystallographic methods. The final model was refined to conventional and free crystallographic R factors of 18.4% and 23.2%, respectively (Table I). The web-based K2SA (http://zlab.bu.edu/k2/) program was used for structural superposition and RMSD calculations. The MDB (http://metallo.scripps.edu/) web server was used for calcium-binding site analysis. PyMOL (http://www.pymol.org/) was used for generating figures. There are three mutations in the structure of Ca dodecin due to PCR artifact: (1) insertion of Val between Met1 and Ser2, (2) A68S, and (3) R71L. These did not affect calcium binding or oligomerization, as they are away from both intersubunit and trimer–trimer interfaces. Electron density for N and C-terminal residues in some subunits (B-1; C-1; D-1, 69-71; E-1; J-1, 70-71; K-1, 69-71) are missing, and the model could not be built for those residues.

Single-particle electron microscopy

Purified Ca dodecin was diluted to 0.05 mg/mL in a buffer containing 20 m*M* Tris-HCl pH 8.0 and 10 m*M* NaCl. The specimens were prepared according to Valentines *et al*.[38] and negatively stained using an aqueous solution of 2% uranyl acetate. Micrographs were recorded on a JEOL 1200EX transmission electron microscope operating to 100 kV at a calibrated magnification of 48, 240. Micrographs were digitized with the Leafscan 45 microdensitometer using a 10 μm scan step resulting in 2.1 Å/pixel at the specimen level and the images were processed using the EMAN single particle analysis package. Reference-free classification were performed on 3900 particles from micrographs with similar defocus values that were low passed filtered to remove special frequencies below 10 Å. The projections observed on the carbon support film, as well as the class averages, lack any views that could indicate an alternative oligomeric form. In fact, all the class averages show spherical particles with a central stain-filled cavity indicating a redundancy of projections consistent with the high symmetry seen in the crystal structure and diminishing the possibility of preferential orientation on the support film.

ICP-OES and atomic absorption spectroscopy

After passing through the gel-filtration column, the native Ca dodecin was used for trace metal analysis. In case of the N-terminal His_6-tagged protein, the His_6 tag was removed using thrombin before passing through gel filtration column. Chelex-100 treated water was used for making the buffers used for the column chromatography. The pooled fractions from gel filtration chromatography were then dialyzed against a buffer containing 25 m*M* Tris-HCl pH 8.0, 10 m*M* NaCl, and 25 g of treated Chelex-100 resin before metal analysis by spectroscopy. Protein samples were digested in nitric and hydrochloric acids, diluted twice with deionized water, and analyzed using CirOS EOP (end-on plasma, or axial viewing), ICP-OES (Spectro Analytical Instruments, Fitchburg, MA), a Burgener T2002 Teflon nebulizer, and a quartz cyclonic spray chamber with baffle accessories. The ytterbium (Yb) was used as an internal standard with external calibration. Calibration standards were prepared from individual element standards, and calibration verification standards

were prepared from certified multielement solutions. A peristaltic pump was used to mix the sample stream with a standard solution at a ratio of ~3:2 and then passed onto the nebulizer. The standard solutions containing 1 ppm of gold (Au), indium (In), and ytterbium (Yb) were used as internal standards.

Dynamic light scattering

The DLS data was collected using Zetasizer Nano-S (Malvern Instruments, UK). The spectra was recorded for varying concentrations of Ca dodecin ranging from 0.5, 1, 1.5, and 2 mg/mL with the corresponding Z values 6.98, 6.96, 6.77, and 6.9 nm, respectively.

Sequence analysis and homology modeling

The Ca dodecin protein sequence was used to pull out homologous sequences from the database of nonredundant protein sequences using BLAST. ClustalW was used for multiple sequence alignment (http://www.biologyworkbench.org). A representative set of protein sequences from the alignment was selected to generate a homology model using the SWISS-MODEL server (http://swissmodel.expasy.org). Crystal structures of Ca dodecin and hsDodecin were used as a template for homology based automated model building.

Acknowledgment

The authors thank Linda Fischer (late) for her excellent support; Bryan Lattin and Dr. Bob Taylor of trace element laboratory, TAMU for ICP-OES analysis; Matthew Ward, Shradda Vora, Elizabeth Caronna, and Stephanie Swanson, for technical assistance; Drs. Giedroc and Sunbae for help with AAS; Drs. Bernard Rupp and M. Hardings for useful discussions on the calcium coordination; and Leslie Nicosia, Tracey Musa, and the Sacchettini lab members for critical reading of the article.

References

1. Berridge MJ, Lipp P, Bootman MD (2000) The versatility and universality of calcium signalling. Nat Rev Mol Cell Biol 1:11–21.
2. Clapham DE (1995) Calcium signaling. Cell 80: 259–268.
3. Rigden DJ, Galperin MY (2004) The DxDxDG motif for calcium binding: multiple structural contexts and implications for evolution. J Mol Biol 343:971–984.
4. Gerke V, Creutz CE, Moss SE (2005) Annexins: linking Ca^{2+} signalling to membrane dynamics. Nat Rev Mol Cell Biol 6:449–461.
5. Norris V, Chen M, Goldberg M, Voskuil J, McGurk G, Holland IB (1991) Calcium in bacteria: a solution to which problem? Mol Microbiol 5:775–778.
6. Herbaud ML, Guiseppi A, Denizot F, Haiech J, Kilhoffer MC (1998) Calcium signalling in *Bacillus subtilis*. Biochim Biophys Acta 1448:212–226.
7. Holland IB, Jones HE, Campbell AK, Jacq A (1999) An assessment of the role of intracellular free Ca^{2+} in *E. coli*. Biochimie 81:901–907.
8. Dominguez DC (2004) Calcium signalling in bacteria. Mol Microbiol 54:291–297.
9. Michiels J, Xi C, Verhaert J, Vanderleyden J (2002) The functions of Ca^{2+} in bacteria: a role for EF-hand proteins? Trends Microbiol 10:87–93.
10. Rigden DJ, Jedrzejas MJ, Moroz OV, Galperin MY (2003) Structural diversity of calcium-binding proteins in bacteria: single-handed EF-hands? Trends Microbiol 11:295–297.
11. Rigden DJ, Jedrzejas MJ, Galperin MY (2003) An extracellular calcium-binding domain in bacteria with a distant relationship to EF-hands. FEMS Microbiol Lett 221:103–110.
12. Yonekawa T, Ohnishi Y, Horinouchi S (2005) A calmodulin-like protein in the bacterial genus *Streptomyces*. FEMS Microbiol Lett 244:315–321.
13. Anantharaman V, Aravind L (2004) The SHS2 module is a common structural theme in functionally diverse protein groups, like Rpb7p, FtsA, GyrI, and MTH1598/TM1083 superfamilies. Proteins 56:795–807.
14. Bieger B, Essen LO, Oesterhelt D (2003) Crystal structure of halophilic dodecin: a novel, dodecameric flavin binding protein from *Halobacterium salinarum*. Structure 11:375–385.
15. Grininger M, Zeth K, Oesterhelt D (2006) Dodecins: a family of lumichrome binding proteins. J Mol Biol 357: 842–857.
16. Grininger M, Staudt H, Johansson P, Wachtveitl J, Oesterhelt D (2009) Dodecin is the key player in flavin homeostasis of archaea. J Biol Chem 284: 13068–13076.
17. Meissner B, Schleicher E, Weber S, Essen LO (2007) The dodecin from *Thermus thermophilus*, a bifunctional cofactor storage protein. J Biol Chem 282: 33142–33154.
18. Einspahr H, Bugg CE (1980) Geometry of calcium water interactions in crystalline hydrates. Acta Cryst B36:264–271.
19. Katz AK, Glusker JP, Beebe SA, Bock CW (1996) Calcium ion coordination: A comparison with that of beryllium, magnesium, and zinc. J Am Chem Soc 118: 5752–5763.
20. Dudev T, Lim C (2003) Principles governing Mg, Ca, and Zn binding and selectivity in proteins. Chem Rev 103:773–788.
21. Harding MM (2001) Geometry of metal-ligand interactions in proteins. Acta Cryst D57:401–411.
22. Berkovitch F, Behshad E, Tang KH, Enns EA, Frey PA, Drennan CL (2004) A locking mechanism preventing radical damage in the absence of substrate, as revealed by the X-ray structure of lysine 5,6-aminomutase. Proc Natl Acad Sci USA 101:15870–15875.
23. Barnham KJ, McKinstry WJ, Multhaup G, Galatis D, Morton CJ, Curtain CC, Williamson NA, White AR, Hinds MG, Norton RS, Beyreuther K, Masters CL, Parker MW, Cappai R (2003) Structure of the Alzheimer's disease amyloid precursor protein copper binding domain. A regulator of neuronal copper homeostasis. J Biol Chem 278:17401–17407.
24. Amara RR, Satchidanandam V (1997) Differential immunogenicity of novel *Mycobacterium tuberculosis* antigens derived from live and dead bacilli. Infect Immun 65:4880–4882.
25. Amara RR, Shanti S, Satchidanandam V (1998) Characterization of novel immunodominant antigens of

Mycobacterium tuberculosis. Microbiology 144:1197–1203.
26. Houghton RL, Lodes MJ, Dillon DC, Reynolds LD, Day CH, McNeill PD, Hendrickson RC, Skeiky YA, Sampaio DP, Badaro R, Lyashchenko KP, Reed SG (2002) Use of multiepitope polyproteins in serodiagnosis of active tuberculosis. Clin Diagn Lab Immunol 9:883–891.
27. Mattow J, Schaible UE, Schmidt F, Hagens K, Siejak F, Brestrich G, Haeselbarth G, Müller EC, Jungblut PR, Kaufmann SH (2003) Comparative proteome analysis of culture supernatant proteins from virulent *Mycobacterium tuberculosis* H37Rv and attenuated *M. bovis* BCG Copenhagen. Electrophoresis 24:3405–3420.
28. Weldingh K, Rosenkrands I, Okkels LM, Doherty TM, Andersen P (2005) Assessing the serodiagnostic potential of 35 *Mycobacterium tuberculosis* proteins and identification of four novel serological antigens. J Clin Microbiol 43:57–65.
29. Otwinowski Z, Minor W, Processing of X-ray diffraction data collected in oscillation mode. In: Carter CW, Jr., Sweet RM, Eds. (1997) Methods in enzymology, volume 276: Macromolecular crystallography, part A. New York: Academic Press, pp307–326.
30. Hendrickson WA (1991) Determination of macromolecular structures from anomalous diffraction of synchrotron radiation. Science 254:51–58.
31. Sheldrick GM (2008) A short history of SHELX. Acta Cryst A64:112–122.
32. Vonrhein C, Blanc E, Roversi P, Bricogne G (2007) Automated structure solution with autoSHARP. Methods Mol Biol 364:215–230.
33. McRee DE, Israel M (2008) XtalView, protein structure solution and protein graphics, a short history. J Struct Biol 163:208–213.
34. Brunger AT (2007) Version 1.2 of the crystallography and NMR system. Nat Protoc 2:2728–2733.
35. Murshudov GN, Vagin AA, Dodson EJ (1997) Refinement of macromolecular structures by the maximum-likelihood method. Acta Cryst D53:240–255.
36. Reddy V, Swanson SM, Segelke B, Kantardjieff KA, Sacchettini JC, Rupp B (2003) Effective electron-density map improvement and structure validation on a Linux multi-CPU web cluster: the TB Structural Genomics Consortium bias removal web service. Acta Cryst D59:2200–2210.
37. Collaborative Computational Project, Number 4 (1994) The CCP4 suite: programs for protein crystallography. Acta Cryst D50:760–763.
38. Valentine RC, Shapiro BM, Stadtman ER (1968) Regulation of glutamine synthetase. XII. Electron microscopy of the enzyme from *Escherichia coli*. Biochemistry 7:2143–2152.